AIMS Animal Science, 2 (1): 35–52.
DOI: 10.3934/aas.2026004
Received: 01 January 2026
Revised: 19 March 2026
Accepted: 07 May 2026
Published: 19 May 2026

https://www.aimspress.com/journal/aas

Research article

Berberine regulates cellular lipid accumulation, oxidative stress, and cell proliferation by modulating Lrrc58a in sodium palmitate-induced Zebrafish hepatocyte

Xuzhuo Wang[1,2], Ho Chong Kin Jacky[3,4,5], Botelho FP[3,4], Yicheng Che[1], Zhaochu Sun[1] and Weina Xu[1,5,*]

[1] Shanghai Key Laboratory for Veterinary and Biotechnology, School of Agriculture and Biology, Shanghai Jiao Tong University, Dongchuan Road, 800, Shanghai 200240, China.
[2] Department of Engineering, Durham University, Stockton Road, DH1 3LE, Durham, United Kingdom.
[3] Faculty of Health Sciences, University of Saint Joseph, Estrada Marginal da Ilha Verde,14-17, Macao, China.
[4] Macao Observatory for Social Development, University of Saint Joseph, Estrada Marginal da Ilha Verde,14-17, Macao, China.
[5] USJ-Kong Hon Academy for Cellular Nutrition, University of Saint Joseph, Estrada Marginal da Ilha Verde,14-17, Macao, China.

***Correspondence:** Email: xuweina@sjtu.edu.cn.

Abstract: We aimed to explore the function of a newly gene Leucine-rich repeat-containing 58a (Lrrc58a) and investigated beberine (BBR) regulate cell physiology by altering Lrrc58a expression in zebrafish hepatocytes (ZFL). Using small interfering RNA (siRNA) interference, the effect of Lrrc58a knockdown on lipid accumulation, oxidative stress, cell apoptosis, and autophagy in ZFL were investigated. Then, four groups, control (CON), a sodium palmitate (SP) treatment group, a beberine (BBR) treatment group, and a sodium palmitate/berberine (SP+BBR) treatment group, were set. The results revealed that Lrrc58a-knockdown cells had increased lipid accumulation, ROS content, cell apoptosis, and autophagy. Compared with the control group, SP treatment suppressed Lrrc58a mRNA expression accompanied by a similar phenotype with the si-Lrrc58a group, while BBR treatment enhanced Lrrc58a mRNA expression and reversed the process. Mechanistically, Lrrc58a knockdown increased lipid accumulation by inhibiting extracellular signal-regulated kinase (ERK), enhanced ROS accumulation by activating c-Jun N-terminal kinase (JNK),

and led to cell apoptosis and autophagy by inhibiting the mammalian target of rapamycin (mTOR). In conclusion, berberine may affect physiological processes such as intracellular lipid accumulation, oxidative stress, cell apoptosis, and autophagy by altering Lrrc58a gene-level changes.

Keywords: Berberine; Lrrc58a; cellular physiology and metabolism

1. Introduction

It is well documented that fat excess deposition in non-adipose tissues (such as liver, heart, skeleton muscle, and pancreas tissue) initiates tissue damage, thus leading to the increase of the risk of metabolic syndrome and, in turn, enhancing liver steatosis and causing other syndromes [1,2]. Exogenous nutrient manipulation can reverse the process. Traditional Chinese medicine has exhibited multiple pharmacological activities, including reducing liver lipid excess deposition, improving antioxidant capacity, and associated diseases in mammals [3]. BBR, a critical natural isoquinoline alkaloid extract from Chinese herbal medicine, has exhibited effects on reducing liver damage [4], lipid metabolism [5], ameliorating body inflammation [6], and cell apoptosis [7,8] over the past two decades. Similarly, our previous studies revealed that BBR addition inhibited lipid excess deposition and the progression of oxidative stress, reduced apoptosis, and enhanced the immunity of fish fed a high-fat diet *in vivo* and *in vitro* [9–11]. However, the process by which BBR regulates the improvement of physiological state is poorly understood. To elucidate this process, m6A Methylation and transcriptome Merip-Seq sequencing on zebrafish hepatocyte treated with BBR or/and SP (sodium palmitate) was carried out. The result showed that BBR could change cellular m6A RNA methylation level, and a new gene, Lrrc58a (LRR containing 58a), was screened out from differentially expressed genes ($p < 0.05$, Fc≥2) (Table S1, [12]).

Leucine-rich repeat (LRR), a widespread and conserved domain in proteins associated with innate immunity, has been found in proteins of all life forms, ranging from viruses to eukaryotes [13]. LRRs are 20–29 residue sequence motifs, and domains containing tandems of two or more LRRs form the continuously expanding LRR superfamily [14,15]. The structure of LRR proteins and domains provides a common structural framework for protein–protein interactions [15]. LRR-containing proteins in intracellular, extracellular, and membrane attachment sites have shown extensive functional diversity, involving enzyme inhibition, RNA processing, cell growth, cell adhesion, signal transduction, and innate immunity [14,16,17]. The biological function of LRR in immunity is gradually emerging [13,18,19], but limited research has been undertaken on its role in lipid metabolism.

Lrrc58a belongs to the LRR superfamily and is a 39.7-kD LRR-containing protein that is highly conserved. It encodes an expressed 351-amino-acid protein that contains eight leucine-rich repeats (LRRs) in its C-terminal domain, which has 58.4% similarity to gene Lrrc58 (*Homo sapiens*) (Figure S1). However, few researchers have reported the function and the mechanism of Lrrc58a; thus, the study was performed to explore the gene function. Lrrc58a was knocked down by si-RNA to understand the role of Lrrc58a in the cellular physiological and metabolic process. Then, we detected Lrrc58a knockdown-induced intracellular lipid accumulation, oxidative stress, autophagy, and apoptosis and verified that nutrient intervention could affect these physiological processes by altering Lrrc58a expression.

2. Materials and methods

2.1. Cell line culture

The ZFL cell line (ATCC® CRL-2643) was purchased from the American Tissue Culture Collection (ATCC, Manassas, VA, USA). The complete growth medium used for cell culture was made from 20% DMEM medium, 30% DMEM/F12 medium, 50% Leibovitz's L-15 medium, the mixture containing 5% fetal bovine serum, 50 ng/ml epidermal growth factor, 10 μg/ml insulin, and 1% penicillin–streptomycin antibiotics purchased from Gibco. The flasks were maintained at 28°C in a cell incubator with 5% CO_2. Cells were passaged at a ratio of 1:2 when hepatocytes were grown to 70–80% confluence.

2.2. N6-methyladenosine (m6A) level detection

m6A modifications on Lrrc58a genes were determined using Genseq® MeRIP m6A Kit (Cat#GS-ET-001)) following the manufacturer's instructions. RNA samples were fragmented (~200 nt), and 1–3ug fragmented RNA was saved as an input sample. Then, immunoprecipitation magnetic beads were prepared, and the immunoprecipitated reaction was performed. The obtained RNA samples were eluted with LB Buffer and HS Buffer, respectively. Thereafter, the eluted RNA samples were purified twice with RLT Buffer and 75% ethanol. Finally, The MeRIP RNA was analyzed with the corresponding input RNA by quantitative RT-PCR.

2.3. Total RNA extraction, reverse transcription, and Real-time PCR

Total cellular RNA was extracted, reverse transcribed, and the expression level of genes was detected by real-time fluorescence quantitative PCR as described previously [12]. Total RNA was extracted using an RNA Kit (Omega, United States) following the manufacturer's instructions under required aseptic conditions. Each RNA sample's quality, integrity, and concentration were determined by 1% agarose gel electrophoresis and a NanoDrop ND-2000 spectrophotometer (Thermo Fisher Scientific, United States). Then, the reaction solution was prepared on ice and mixed thoroughly. The configured mixture was divided into reaction tubes (25 uL reaction system). Next, the qPCR was carried out on a CFX96 Real-Time PCR detection system (Bio-Rad), and the specific reaction conditions were performed. Quantification of the target gene transcripts in each sample was normalized with β-actin expression calculated by the $2^{-\triangle\triangle Ct}$ method. Normalized gene expression for the control group was set at 1. The primers of all the genes were synthesized by Personal Gene Technology Co., Ltd. (Shanghai, China) and are listed in Table S1.

2.4. Transfection and cell treatment

siRNAs for Lrrc58a or negative control (mimic--NC) duplex were designed and provided by GenePharma (Shanghai, China). The siRNA sequences were as follows: siRNA-Lrrc58a, sense: 5'-CGGCCAAUCUGAUCUAUUATT-3', antisense: 5'-UAAUAGCAUCAGAUUGGCCGTT-3'; siRNA was transfected with Lipofectamine TM 2000 transfection kit (Thermo Fisher) according to the manufacturer's protocol and transfected when the cells met at 70% confluent in six-well plates. Transfection was repeated three times. Sodium Palmitate or/and Berberine treatment were used to regulate mRNA Lrrc58a expression.

Then four groups were designed: control (CON), a sodium palmitate (SP) treatment group, beberine (BBR) treatment group, and sodium palmitate/berberine (SP+BBR) treatment group. CON group cells were culture with complete growth medium. For the SP group, the cells were exposed to complete work media containing 0.25 mM SP for 24 hours. For BBR group, the cells were treated with 25 μM BBR working solution (solvent 0.1% DMSO) for 6h. For SP +BBR group, the cells were exposed to 0.25 mM SP working solution for 24 hours and the changed BBR working solution (25 μM) for 6h [12].

2.5. Cell viability assay

According to the manufacturer's instructions, the ZFL cell viability was detected by cell counting kit-8 assay (Dojindo). ZFL were seeded in 96-well plates (1×10^4 cells/well) for 24h. After treatment, CCK8 reagent was added to each well and incubated for 2 h. Then, a microplate reader (Synergy H1; BioTek) was used to assess cell viability (at 450 nm), and the errors caused by the differences in the cell numbers in each group in the fluorescence intensity assay were corrected versus the CCK-8 signal.

2.6. Oil red O staining

Intracellular lipid droplets were detected by oil red O (Sigma-Aldrich). ZFL were seeded in 6-well plates (3×10^5 cells/well) for 24h. After treatment, cells were washed with DPBS twice and fixed with 4% formaldehyde at 4°C for 1h, followed by 0.5% oil red O staining for 45 minutes at 28°C. Once the staining finished, cells were washed with DPBS to remove the residual dye. Then, cells were observed through an inverted microscope, and pictures were taken (TE2000--E; Nikon).

2.7. Cellular biochemical parameters assay

After treatment, the original cell culture medium was discarded, followed by rinsing with DPBS. Then, 100 μL cell lysis solution was added to lyse the cells fully. For lipid accumulation, intracellular TG and TC content were measured using commercial kits (Nanjing, Jiangsu, China) at 510 nm (Synergy H1; BioTek).

2.8. ROS content

DCFH-DA probe (Beyotime Biotechnology) was used to detect intracellular reactive oxygen species (ROS) content. After treatment, cells were rinsed with DPBS three times, incubated with DCFH-DA probe for 30 min, and rinsed with DPBS. Then, a microplate reader was used to determine the fluorescence intensity at an excitation wavelength of 488 nm and an emission wavelength of 525 nm. ROS fluorescence photographs were also taken.

2.9. Oxidative stress assay

For oxidative stress indicators, after treatment, the supernatant of cell lysis was measured for total antioxidant capacity (T-AOC), superoxide dismutase (SOD) activity, and glutathione (GSH) content. The contents and enzyme activities were presented as the ratio of values to protein concentration. The content of protein in each sample was determined by a BCA Protein Assay Kit. These biochemical parameters were measured using commercial kits (Nanjing, Jiangsu, China) according to the manufacturers' instructions.

2.10. Cell apoptosis

Annexin V-Fluorescein isothiocyanate (FITC)/ propidium iodide (PI.) apoptosis assay kit (Beyotime Biotechnology) was used to quantify the percentage of cells undergoing apoptosis. Cells were collected at 1×10^5 cells per tube after centrifugation (×1000*g*, 5min) and then washed twice with ice-cold DPBS. Next, cells were resuspended in 195 uL Annexin V -FITC binding buffer followed by 5 uL Annexin V-FITC and 10 uL of PI. After incubation for 15 min at room temperature in the dark, cell apoptosis was detected by flow cytometry within 1h. The upper left quadrant represented a mechanically injured cell, and the upper right quadrant was a late apoptotic cell. The lower left quadrant was a normal cell, and the lower right quadrant was an early apoptotic cell. In this experiment, the proportion of the upper right quadrant(Q2) + the lower right quadrant (Q4) was used as the percentage of apoptotic cells. The data were analyzed using FlowJo software version 7.6.1.

Apoptosis rate (%) = number of apoptotic cells/total number of cells × 100%.

2.11. Transmission electron microscopy analysis

For transmission electron microscopy (TEM) analysis, ZFL were seeded in a 10cm petri dish (3×10^6 cells/dish) for 24h. After treatment, cells were scraped off directly, and the cell suspension was transferred to the centrifuge tube. Cells were fixed with 2.5% glutaraldehyde fixative for 6–8 h and then washed with DPBS. Then, the cells were postfixed with 1 % osmium tetroxide for 2h and progressively alcohol--dehydrated, embedded, and polymerized for 48 hours at 60°C. Next, representative sections (60–70 nm) were prepared and double-stained with 3% uranyl acetate and lead citrate. Imaging of sections was completed with a transmission electron microscope (Talo L120C G2; Thermo).

2.12. Western blot

After treatment, the cells were washed with ice-cold DPBS and then lysed for 30 min with RIPA cell lysis solution. The total protein concentration was determined by the BCA method. The equal quantities of protein (30 ug) were separated by 10% SDS-PAGE and transferred to the PVDF membranes (200 mA 2 h). Antibodies to LC3B, ATG7, Beclin1, ERK, p-ERK, PI3K, p-PI3K, m-TOR, p-m-TOR, JNK, p-JNK (1:1000), and α-tubulin (1:2000) were incubated with blots overnight at 4°C in the buffer recommended and then washed with TBST. Next, the membranes were incubated with HRP-conjugated secondary antibody (1:2000) for 2h at room temperature and then washed with TBST. The protein bands were then visualized using ECL reagents according to the manufacturer's protocol. Image J software was used to analyze the fold-changes of protein levels. The protein bands were normalized to those of α-tubulin.

2.13. Statistical analysis

Statistical differences between the groups were analyzed using One-way analysis of variance (ANOVA) and checked for normality and homogeneity of variance before analysis. Duncan's multiple range test was applied when a significant difference was observed between groups. All results were presented as mean ± standard error (X ± SEM) from at least three independent experiments. $p < 0.05$ indicated a statistically significant difference.

3. Results

3.1. Biological Function of the Lrrc58a Assay

As a newly discovered gene, the literature has reported the function of Lrrc58a. Initially, Lrrc58a was assayed to validate the DEG data (Figure 1A.B). Then, the function of the gene was explored using siRNA (si-Lrrc58a) in ZFL, and its transfection efficiency was verified by qRT-PCR. The results showed that the Lrrc58a knockdown efficiency ($P < 0.05$) reached >50% at 36h after transfection (Figure 1C).

3.1.1. Intracellular lipid accumulation and oxidative stress

We first explored the intracellular lipid contents to investigate the relationship between lipid accumulation and Lrrc58a expression. As visualized by ORO staining, TG, and TC contents, Lrrc58a knockdown remarkably ($P < 0.05$) aggravated lipid accumulation *in vitro* compared to the control group (Figure 1D-F). Compared with the control group, lipolysis-related gene PPARα and ATGL of the si-Lrrc58a group were significantly ($P < 0.05$) decreased. No difference was observed in the FAS and ACC genes (Figure 1G). As seen in Figure 1, compared with the control group, the intracellular ROS content of the si-Lrrc58a group was significantly ($P < 0.05$) increased, indicating apparent oxidative stress occurred (Figure 1H.I). Additionally, major antioxidant indicators, T-AOC and GSH contents, were significantly ($P < 0.05$) decreased. SOD activity of the si-Lrrc58a group was slightly increased (Figure 1G-L).

3.1.2. Cell apoptosis and autophagy

A growing amount of evidence shows that LRR superfamily proteins affect cell proliferation and apoptosis. Therefore, the relationship between Lrrc58a and cell apoptosis was next performed. As displayed in Figure 2, compared with the control group, cell apoptosis rate determined by flow cytometry (Figure 2A.B) and relative mRNA Bax expression determined by qRT-PCR (Figure 2D) in the si-Lrrc58a group were significantly ($P < 0.05$) increased. Moreover, cell viability was significantly decreased (Figure 2C). The relative mRNA of ATG 7, Beclin1, and LC3B expression were increased ($P < 0.05$) compared to those of the control group (Figure 2E). In addition, western blot analysis showed that the protein expression of ATG 7, Beclin1, and LC3B in the different groups was consistent with the mRNA level (Figure 2F.H). Moreover, ultrastructural analysis by TEM further showed that cells of the si-Lrrc58a group were severely vacuolated: Crushed and deformed nucleoli, apparent autophagic vesicles were observed (Figure 2I).

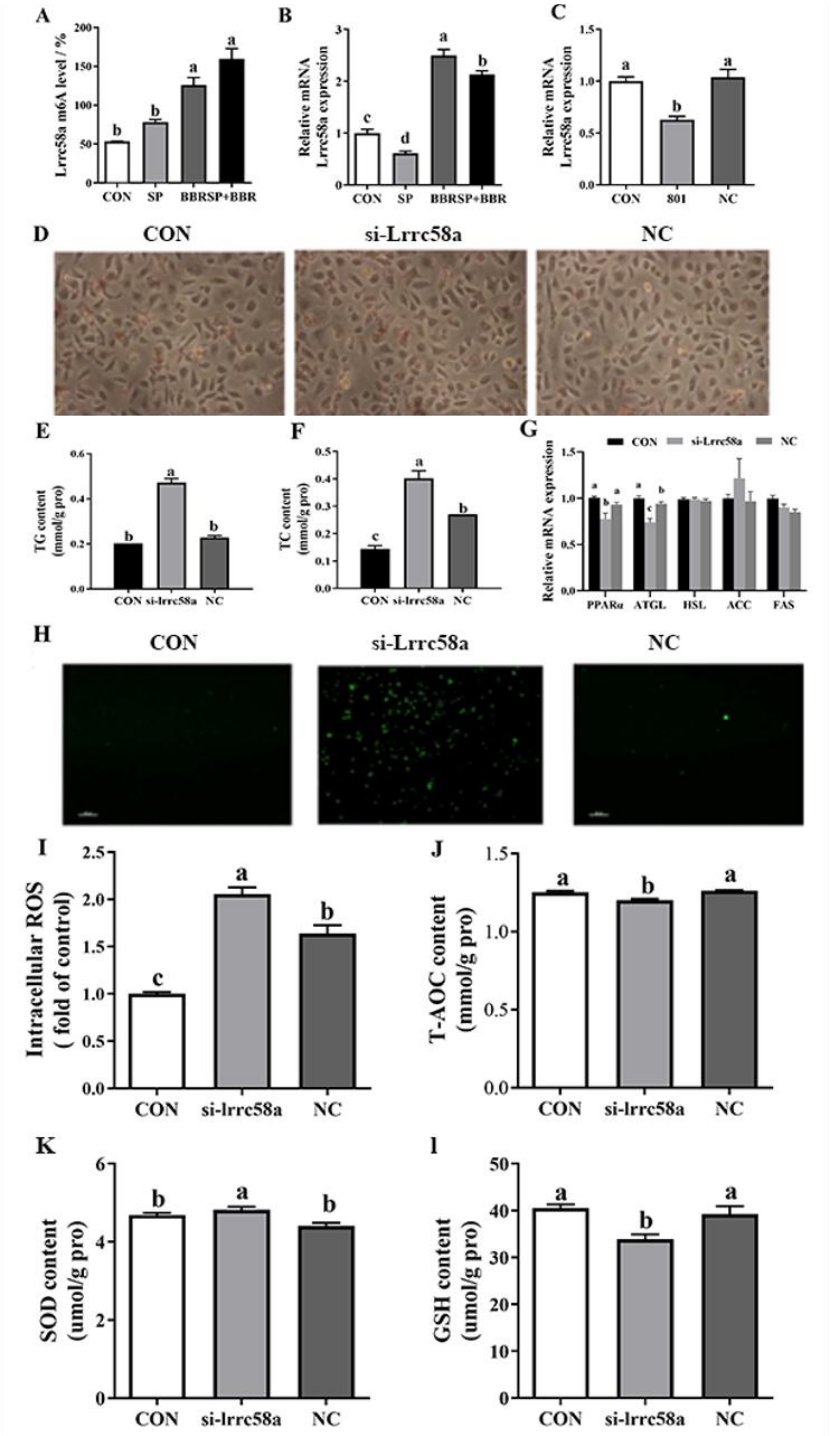

Figure 1. Intracellular lipid accumulation and oxidative stress. **(A)** m6A methylation level analysis of Lrrc58a, performed by immunomagnetic bead. **(B)** qRT-PCR analysis of Lrrc58a. **(C)**qRT-PCR analysis of Lrrc58a knockdown efficiency at 36h. **(D)** ORO staining. **(E)** TG content. **(F)** TC content. **(G)** qRT-PCR analysis of gene expression of lipogenesis and lipolysis. (**H**) Detection of ROS production with DCFH-DA staining (**H**, scale bar, 10 μm). (**I)** The mean intensity of green fluorescence represents the level of ROS in the cells. (**J-L)** Detection of major intracellular antioxidant enzyme activities; **J.** T-AOC. **K.** SOD, and (**L.** GSH. The experiment was repeated three times (n = 3), and the different letters indicate a significant difference ($P < 0.05$). β-actin is the internal control in qRT-PCR analysis.

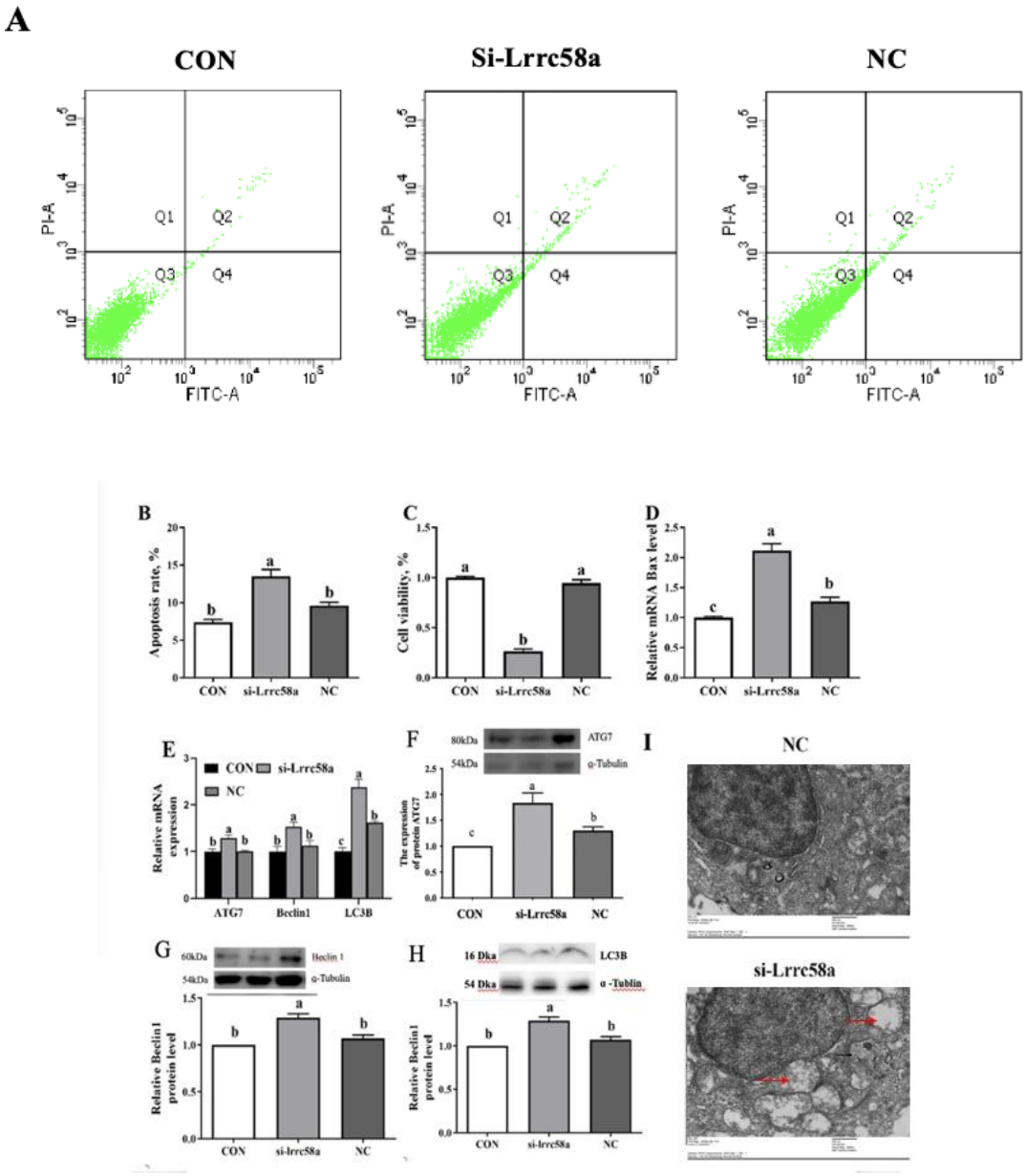

Figure 2. Cell apoptosis and autophagy. (**A,B**) Detection of apoptosis in ZFL cells by Annexin-V/PI double-staining followed by flow cytometric analysis. The upper right (Q2) and lower right areas (Q4), which represents the percentage of late apoptosis and early apoptosis, are analyzed. **(A)** Representative cytograms of apoptosis. **(B)** Quantification of cell apoptosis. (**C)** Detection of cell viability by CCK-8. (**D)** Relative expression of Bax after treatments. (**E-H)** Detection of qRT-PCR (**E**) and western blot **(F-H)** on the expression levels of ATG7 (**F**), Beclin1(**G**), and LC3B(**H**) protein. **(I)** Transmission electron microscope images of ZFL cell after treatments. The black arrow is the autophagic vacuole; and the red arrow is swollen mitochondria. The experiment was repeated three times (n=3), and the letters indicate a significant difference ($P < 0.05$).

3.1.3. mTOR/ERK/JNK signaling pathway factors assay

Studies have demonstrated that PI3K, ERK, JNK, and mTOR signaling pathways are related to regulating lipid accumulation, oxidative stress, cell apoptosis, and autophagy [20–23]. Therefore, the expression of the above proteins and their phosphorylated proteins were tested. As displayed in Figure 3, the ratio of p- ERK/ ERK and p-mTOR/mTOR were significantly ($P < 0.05$) decreased, and p- JNK/ JNK was increased considerably ($P < 0.05$), while no difference was observed for p-PI3K/ PI3K after Lrrc58a knockdown.

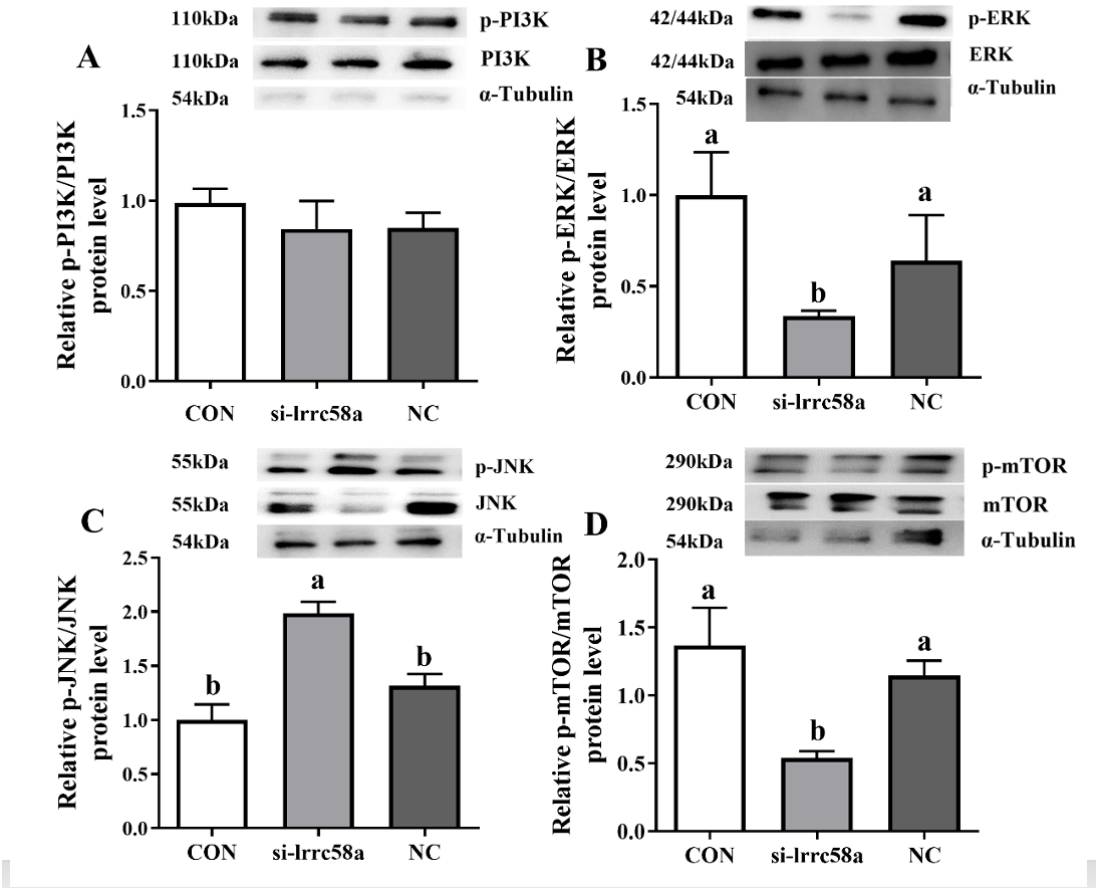

Figure 3. Detection of western blot on the expression levels of p-PI3K, PI3K, p-ERK, ERK, p-JNK, JNK, p-mTOR, and mTOR proteins. The data showed the ratio of p-PI3K/PI3K (**A**), p-ERK/ERK (**B**), p-JNK/JNK (**C**), and p-mTOR/mTOR (**D**). The experiment was repeated three times (n=3), and the letters indicate a significant difference ($P < 0.05$).

3.2. Lipid Accumulation, Oxidative stress, Apoptosis, and Autophagy Assays under SP or BBR treatment

Figure 1 shows that gene Lrrc58a expression of the SP group was significantly ($P < 0.05$) decreased compared with the control group. Moreover, BBR treatment (BBR and SP+BBR group) significantly ($P < 0.05$) enhanced Lrrc58a expression compared with the other two groups (Figure 1B). Comparable results were found in the SP group, with increased ($P < 0.05$) TG/TC content and ROS content and impaired antioxidant capacity, indicating severe lipid accumulation and oxidative stress (Figure 4). In contrast,

BBR/SP+BBR treatment mitigated lipid accumulation and oxidative stress, exhibiting lower ($P < 0.05$) TG/TC content and ROS content (Figure 4).

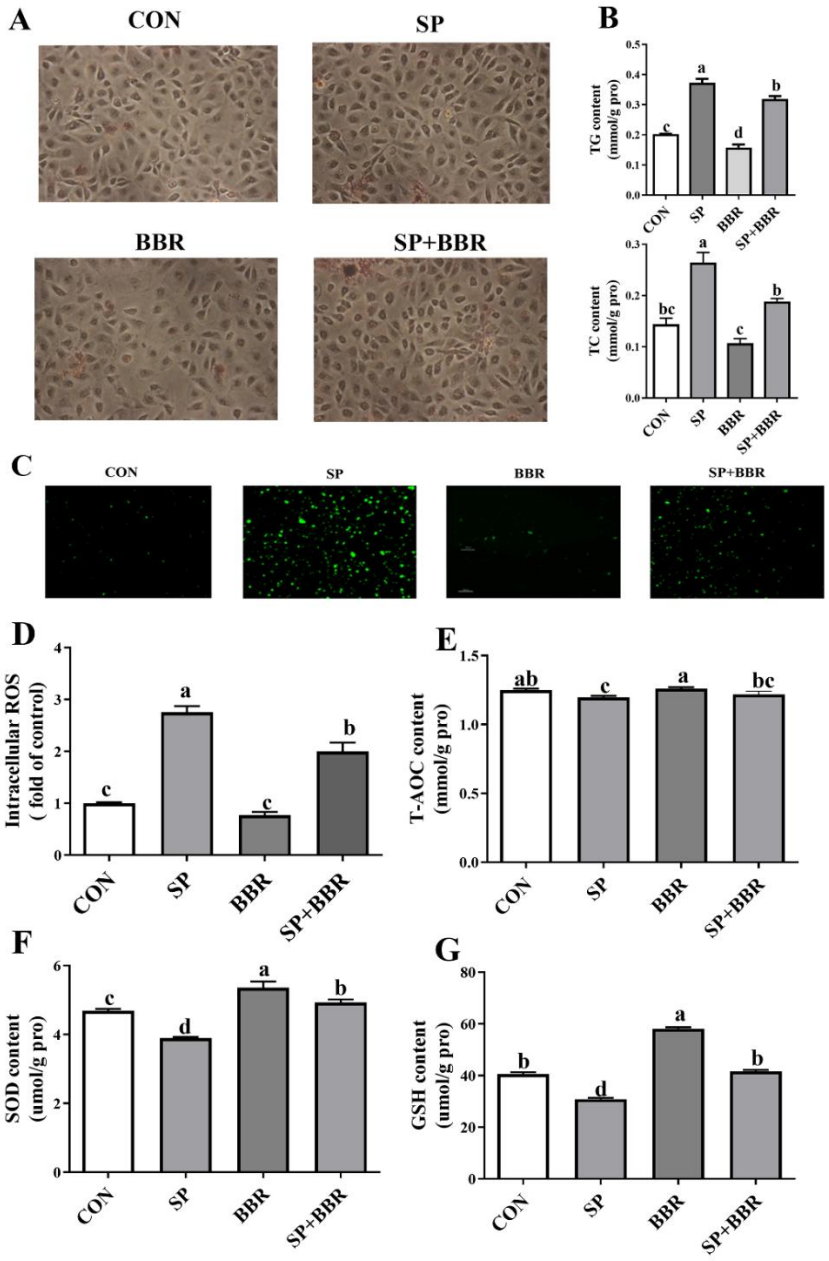

Figure 4. Intracellular lipid accumulation and oxidative stress. **(A)** ORO staining analysis. **(B)** TG and TC content. (**C.D**) Detection of ROS production with DCFH-DA staining (**C**, scale bar, 10 μm). (**D)** The mean intensity of green fluorescence represents the cells' ROS level. (**E-G)** Detection of major intracellular antioxidant enzyme activities (**E.** T-AOC.**F.** SOD) and antioxidant content (**G.** GSH). The experiment was repeated three times (n=3), and the letters indicate a significant difference ($P < 0.05$). Control (CON), ZFL without treatment. Sodium palmitate treatment (SP), ZFL with 0.25 mM Sodium Palmitate treatment. Berberin treatment (BBR), ZFL with 25 μM Berberine treatment. **S**odium palmitate/berberine treatment (SP+BBR), ZFL with 0.25 mM SP and 25 μM BBR treatment.

Compared with the control group, cultured cells of the SP group exhibited higher ($P < 0.05$) cell apoptosis and autophagy factor expressions (Figure 5). The results showed that cell apoptosis and relative mRNA Bax expression significantly ($P < 0.05$) declined in the BBR and SP+BBR groups compared to the SP group (Figure 5A and D). As a consequence, cell viability was significantly ($P < 0.05$) enhanced (Figure 5C). Moreover, major autophagy indicator ATG 7, Beclin1, and LC3B relative mRNA expression were significantly ($P < 0.05$) declined in BBR treatment compared with the SP treatment group (Figure 5E). Western blot analysis showed that the protein expression of ATG 7, Beclin1, and LC3B was consistent with the mRNA level (Figure 5F-G). p-ERK/ ERK, p- JNK/ JNK, and p-mTOR/mTOR protein expressions were determined. Compared with SP, the ratio of p-ERK/ERK or p-mTOR/mTOR in BBR/SP and BBR groups were significantly ($P < 0.05$) enhanced, while p-JNK/JNK ratio was significantly ($P < 0.05$) declined (Figure 6).

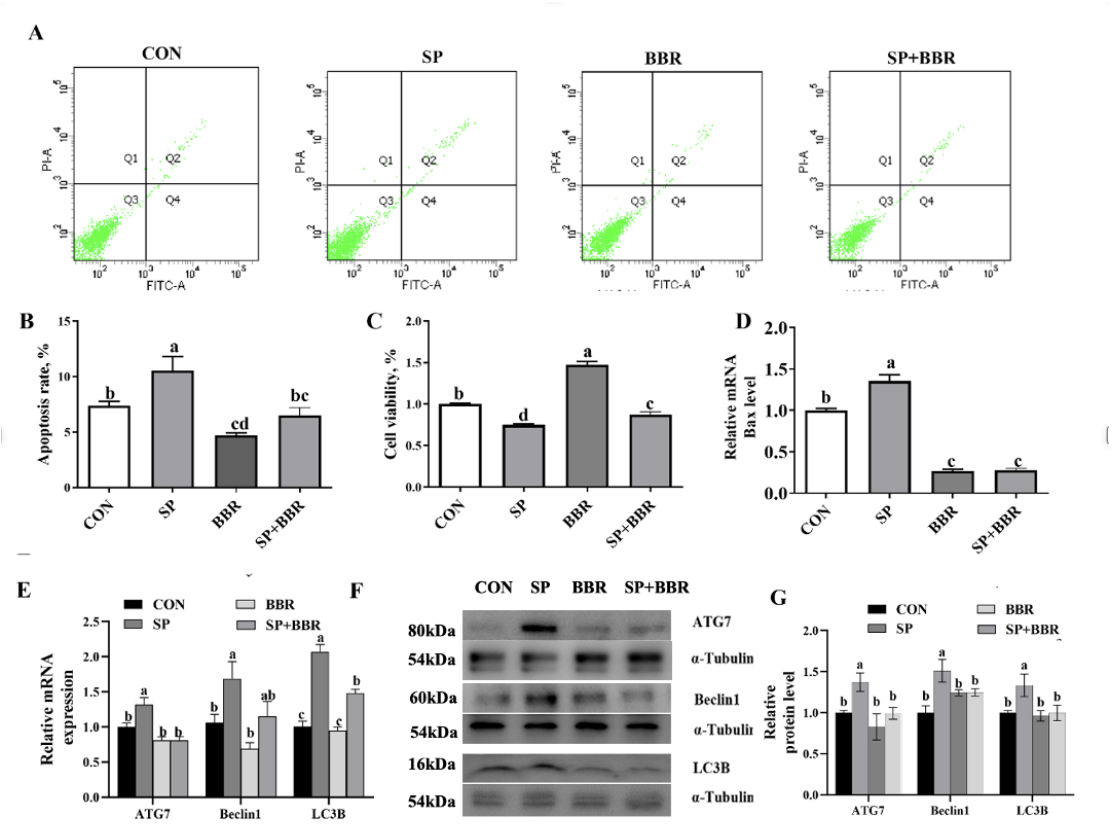

Figure 5. Cell apoptosis and autophagy. (**A,B**) Detection of apoptosis in ZFL cells by Annexin-V/PI double-staining followed by flow cytometric analysis. The upper right (Q2) and lower right areas(Q4), representing the percentage of late and early apoptosis, are analyzed. **(A)** Representative cytograms of apoptosis. **(B)** Quantification of cell apoptosis. (**C**) Detection of cell viability by CCK-8. (**D**) Relative expression of Bax after treatments. (**E-G**) Detection of qRT-PCR (**E**) and western blot **(F-g)** on the expression levels of ATG7, Beclin1 and LC3B(**G**) protein. The experiment was repeated three times (n=3), and the letters indicate a significant difference ($P < 0.05$).

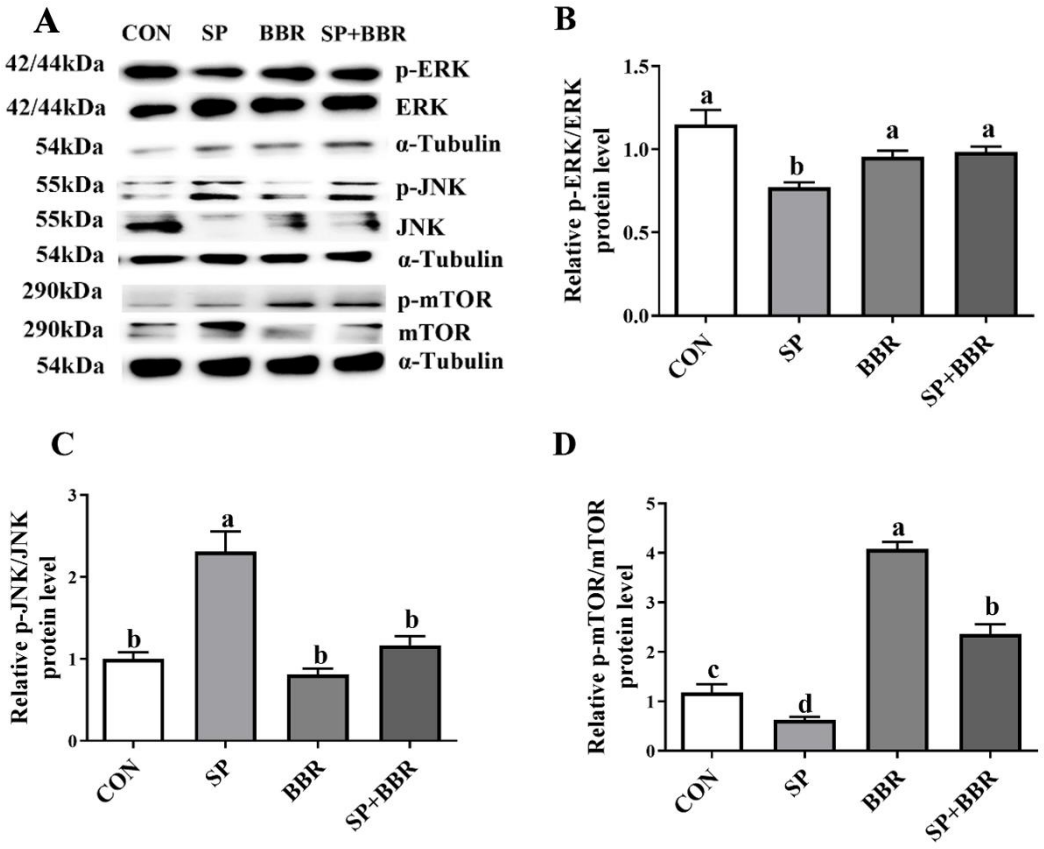

Figure 6. Signaling pathways assay. **A.** Representative images of western blot Detection of western blot on the expression levels of p-ERK, ERK, p-JNK, JNK, p-mTOR, mTOR, and proteins. The data show the ratio of (**B**) p-ERK/ERK, (**C**) p-JNK/JNK, and (**D**) p-mTOR/mTOR. The experiment was repeated three times (n=3), and the letters indicate a significant difference ($P < 0.05$).

4. Discussion

In our previous study, we demonstrated that nutrient manipulation regulated total methylation level [12], and Lrrc58a was screened out from co-analysis of methylation and transcriptome. In this paper, we studied if Lrrc58a is involved in lipid accumulation, oxidative stress, apoptosis, and autophagy processes and change related-key factors, such as ERK, JNK, and mTOR in ZFL.

Lrrc58a, a leucine-rich repeat-containing 58a protein, belongs to the LRR superfamily protein. Moreover, members of the LRR superfamily have been reported to regulate gene expression, cell proliferation, and apoptosis, while researchers have investigated the relationship between LRR and lipid metabolism [14,17,24]. Our study demonstrated that Lrrc58a knockdown induced severe lipid accumulation; similar results were found in the SP group. Therefore, we hypothesized that SP could induces lipid accumulation by inhibiting Lrrc58a expression. After BBR treatment, the TG and TC contents of the BBR and SP+BBR groups decreased simultaneously. Further evidence suggested that Lrrc58a knockdown exacerbated intracellular lipid accumulation by inhibiting the expression of lipolytic genes. These results may point out that the pro-lipolytic effect of BBR may be exerted through Lrrc58a expression changes.

The ERK signaling pathway, one of the MAPK pathways, plays a vital role in regulating lipid metabolism, such as lipid synthesis, oxidative decomposition, and lipid transport [25–27]. Additionally, it has been revealed that ERK induces the expression of lipid metabolism-related genes such as PPAR [23,27]. In our study, Lrrc58a knockdown consistently inhibited the expression of p-ERK protein and, consequently, the expression of downstream genes PPARα and ATGL. On the other hand, BBR-enhanced Lrrc58a expression reversed the above phenomenon and curbed lipid accumulation. Taken together, we suggest that BBR treatment enhances mRNA Lrrc58a expression by elevating the Lrrc58a methylation level, which activates ERK and downstream lipolysis-related gene expression and reduces intracellular lipid accumulation.

In the early stage of intracellular lipid accumulation, cells would accelerate lipid catabolism to maintain intracellular homeostasis, and mitochondria produce a small number of ROS through β-oxidation. When lipid accumulation continues, continuous activation of mitochondrial β-oxidation generates many ROS, damaging mitochondrial function and decreasing ATP production, leading to impaired lipid metabolism and increased lipid accumulation [28,29]. Moreover, there are two major methods for scavenging ROS; enzymes such as SOD and non-enzymatic antioxidants such as GSH [30,31]. SOD, the superoxide enzyme, catalyzes superoxide anion radicals (O^{2-}) into O^2 and H_2O_2, which plays a vital role in maintaining the balance of ROS [30]. Glutathione, a major cellular antioxidant, is recognized as a vital indicator of the degree of oxidative stress. The other is to increase antioxidant capacity by supplementing with exogenous antioxidants [31]. The action of enzymes and non-enzyme systems simultaneously would lead to a better effect in removing ROS and resisting oxidative stress. In this study, under normal conditions, the production and scavenging of ROS are in balance and dynamic changes. However, excessive intracellular fat accumulation could imbalance the REDOX system and increase intracellular ROS content, which induces cellular dysfunction. Therefore, the effect of Lrrc58a knockdown on oxidative stress levels was evaluated. ROS was significantly increased, and antioxidant enzyme activity and antioxidant content were significantly decreased in the si-Lrrc58a and SP groups, indicating the core role of Lrrc58a in cellular oxidative stress. Conversely, BBR treatment effectively mitigated oxidative stress on declined ROS content and increased antioxidant capacity. Herein, increased SOD activity was observed in the BBR group. To our astonishment, SOD activity was also increased in the si-Lrrc58a group, while the GSH level was decreased. The reason for this might be that a certain amount of ROS produced after Lrrc58a knockdown preferentially consumes antioxidants and reduces the damage of ROS to antioxidant enzymes, which stimulates the activity of antioxidant enzymes slightly and leads to a declined total antioxidant capacity. Besides, much literature has reported that BBR has a scavenging ability to quench O^{2-} and NO. Furthermore, BBR upregulated non-enzymatic antioxidant defenses [29,32]. Additionally, researchers have reported that BBR treatment activates AMPK phosphorylation to promote the transcription and activity of the antioxidant gene SOD in response to oxidative stress [32,33]. Thus, we suppose that BBR treatment may promote AMPK phosphorylation through Lrrc58a activation to deal with oxidative stress, which requires further investigation.

More evidence showed that certain ROS levels promote cell proliferation and differentiation. Furthermore, the increased generation and accumulation of ROS exacerbate cellular damage by attacking biofilms, membrane systems, DNA, proteins, and other macromolecules [2,34]. The initiation of apoptosis can be determined by morphological changes such as nuclear fragmentation, chromatin condensation, cell shrinkage, and membrane blistering [35,36]. Consistent with this, Annexin V staining and TEM showed that ZFL cells of si-Lrrc58a began to show an apoptosis phenotype, with a sharp increase in apoptosis rate and a significant rise in pro-apoptotic related genes. After BBR treatment, Lrrc58a expression was enhanced in

hepatocytes, pro-apoptotic genes were significantly reduced, and cell apoptosis was effectively weakened, indicating that Lrrc58a may be a key factor in apoptosis development.

Comparable to apoptosis, autophagy is a conserved physiological phenomenon in eukaryotic that degrades dysfunctional proteins and organelles to counteract stress [37]. This process is pivotal for sustaining cellular metabolism, homeostasis, and genomic integrity; thus, its compromise is a key factor in the pathogenesis of numerous diseases [22,38]. In recent years, many studies have linked LRRC to autophagy. Kunapuli et al. demonstrated that LGI1, a member of the LRR superfamily gene, significantly inhibited cell proliferation and invasion in cells that do not (T98G glioma cell line) express LGI1 endogenously [39]. Xian et al. found that the LRRC59 gene regulates type I interferon signaling by inhibiting SQSTM1/P62-mediated autophagic degradation of pattern recognition receptors [16]. Consistent with these results, we found that Lrrc58a knockdown enhanced the mRNA and protein expression of autophagy factors and accelerated the formation of autophagosomes. These results indicated that the cells undergo a transition from physiological autophagy to pathological excessive autophagy, which affects the function and state of the cells. Moreover, cells of SP treatment-induced low Lrrc58a expression showed excessive autophagy. Conversely, BBR treatment combined with high Lrrc58a expression restored physiological autophagy in the cell. In aggregate, Lrrc58a may be a key factor in regulating autophagy.

JNK, a vital member of the MAPK superfamily, is a crucial regulator of ROS-mediated cell responses with various functions to regulate cellular activities and stress responses [40]. Studies have shown that high levels of ROS can induce autophagy and apoptosis by activating the JNK signaling pathway in human cervical cancer cells and osteosarcoma cells [41]. In addition, the mTOR signaling pathway is a classical pathway that regulates cell proliferation, autophagy, and apoptosis. The accumulation of ROS can also induce autophagy and apoptosis by regulating the mTOR pathway [21]. In our study, Lrrc58a knockdown, intracellular ROS accumulation, JNK and mTOR phosphorylation, apoptosis, and autophagy processes were changed. Moreover, BBR treatment increased JNK and mTOR phosphorylation, inhibiting cell autophagy and apoptosis. Additionally, berberine increased cell Lrrc58a gene expression. Moreover, many researchers have reported that PI3K/Akt and AMPK, as upstream kinases of mTOR, regulate cell proliferation, survival, apoptosis, and autophagy by affecting the phosphorylation of the downstream mTOR signals [42–44]. However, no difference was observed in PI3K phosphorylation levels among groups after the Lrrc58a knockdown, indicating that PI3K was not involved in the Lrrc58a-regulated physiological process.

Therefore, based on the present data, we inferenced that berberine could participate in lipid metabolism, apoptosis, or autophagy through Lrrc58a gene experssion changes. However, in this paper, there was no direct evidence to prove this, whice requires further investigation.

5. Conclusions

In summary, beberin could affect cell physiology and metabolism, including intracellular lipid accumulation, oxidative stress, and autophagy processes through Lrrc58a gene expresion changes. However, a limitation should be acknowledged for this study: It did not provide adequate evidence to support a direct link between berberine activity and the regulation of lrrc58a. Further studies about genes operating within the same regulatory pathway and additional genes or pathway components related to lrrc58a should be investigated.

Use of AI tools declaration

The authors declare they have not used Artificial Intelligence (AI) tools in the creation of this article.

Author Contributions

Weina Xu conceived and designed the experiments. Xuzhuo Wang, Yicheng Che and Zhaochu Sun performed most of the experiments. Xuzhuo Wang responded for data analysis. Ho Chong Kin Jacky and F. P. Botelho provided technical assistance. Weina Xu and Xuzhuo Wang wrote the article. All authors have read and agreed to the published version of the manuscript.

Funding

This work was supported by National Key Research and Development Program of China [grant numbers 2023YFD1301803].

Acknowledgments

This work was jointly supported by grants from the School of Agriculture and Biology, Shanghai Jiao Tong University.

Conflicts of interest

The authors declare no competing interest.

References

1. Samuel VT, Shulman GI (2012) Mechanisms for insulin resistance: Common threads and missing links. *Cell* 148: 852–871. https://doi.org/10.1016/j.cell.2012.02.017
2. Giorgi C, Marchi S, Simoes ICM, et al. (2018) Mitochondria and reactive oxygen species in aging and age-related diseases. *Int Rev Cell Mol Biol* 340: 209–344. https://doi.org/10.1016/bs.ircmb.2018.05.006
3. Zhou M, Deng Y, Liu M, et al. (2021) The pharmacological activity of berberine, a review for liver protection. *Eur J Pharmacol* 890: 173655. https://doi.org/10.1016/j.ejphar.2020.173655
4. Huang CH, Huang ZW, Ho FM, et al. (2018) Berberine impairs embryonic development in vitro and in vivo through oxidative stress-mediated apoptotic processes. *Environ Toxicol* 33: 280–294. https://doi.org/10.1002/tox.22515
5. Ilyas Z, Perna S, Al-Thawadi S, et al. (2020) The effect of Berberine on weight loss in order to prevent obesity: A systematic review. *Biomed Pharmacother* 127: 110137. https://doi.org/10.1016/j.biopha.2020.110137
6. Chen C, Yu Z, Li Y, et al. (2014) Effects of berberine in the gastrointestinal tract—a review of actions and therapeutic implications. *Am J Chin Med* 42: 1053–1070. https://doi.org/10.1142/S0192415X14500669
7. Gaba S, Saini A, Singh G, et al. (2021) An insight into the medicinal attributes of berberine derivatives: A review. *Bioorg Med Chem* 38: 116143. https://doi.org/10.1016/j.bmc.2021.116143
8. Zhou Y, Liu SQ, Yu L, et al. (2015) Berberine prevents nitric oxide-induced rat chondrocyte

apoptosis and cartilage degeneration in a rat osteoarthritis model via AMPK and p38 MAPK signaling. *Apoptosis* 20: 1187–1199. https://doi.org/10.1007/s10495-015-1152-y

9. Chen QQ, Liu WB, Zhou M, et al. (2016) Effects of berberine on the growth and immune performance in response to ammonia stress and high-fat dietary in blunt snout bream *Megalobrama amblycephala*. *Fish Shellfish Immunol* 55: 165–172. https://doi.org/10.1016/j.fsi.2016.05.023
10. Yang SS, Yu CB, Luo Z, et al. (2019) Berberine attenuates sodium palmitate-induced lipid accumulation, oxidative stress and apoptosis in grass carp (*Ctenopharyngodon idella*) hepatocyte in vitro. *Fish Shellfish Immunol* 88: 518–527. https://doi.org/10.1016/j.fsi.2019.02.055
11. Yu C, Zhang J, Qin Q, et al. (2020) Berberine improved intestinal barrier function by modulating the intestinal microbiota in blunt snout bream (*Megalobrama amblycephala*) under dietary high-fat and high-carbohydrate stress. *Fish Shellfish Immunol* 102: 336–349. https://doi.org/10.1016/j.fsi.2020.04.052
12. Zhang M, Liu J, Yu C, et al. (2022) Berberine regulation of cellular oxidative stress, apoptosis and autophagy by modulation of m6A mRNA methylation through targeting the Camk1db/ERK pathway in zebrafish-hepatocytes. *Antioxidants* 11: 2370. https://doi.org/10.3390/antiox11122370
13. Shi Q, Zhang Y, Ni M, et al. (2024) Expression characteristics and inhibitory activity of a leucine-rich repeat (LRR)-only protein in the Chinese mitten crab *Eriocheir sinensis*. *Fish Shellfish Immunol* 145: 109300. https://doi.org/10.1016/j.fsi.2023.109300
14. Bella J, Hindle KL, McEwan PA, et al. (2008) The leucine-rich repeat structure. *Cell Mol Life Sci* 65: 2307–2333. https://doi.org/10.1007/s00018-008-8019-0
15. Kobe B, Kajava AV (2001) The leucine-rich repeat as a protein recognition motif. *Curr Opin Struct Biol* 11: 725–732. https://doi.org/10.1016/S0959-440X(01)00266-4
16. Xian H, Yang S, Jin S, et al. (2020) LRRC59 modulates type I interferon signaling by restraining the SQSTM1/p62-mediated autophagic degradation of pattern recognition receptor DDX58/RIG-I. *Autophagy* 16: 408–418. https://doi.org/10.1080/15548627.2019.1615303
17. Platt CD, Chou J, Houlihan P, et al. (2017) Leucine-rich repeat containing 8A (LRRC8A)-dependent volume-regulated anion channel activity is dispensable for T-cell development and function. *J Allergy Clin Immunol* 140: 1651–1659. https://doi.org/10.1016/j.jaci.2016.12.974
18. Zhan Y, Zhao CS, Qu X, et al. (2023) Identification of a novel amphioxus leucine-rich repeat receptor involved in phagocytosis reveals a role for Slit2-N-type LRR in bacterial elimination. *J Biol Chem* 299: 104689. https://doi.org/10.1016/j.jbc.2023.104689
19. Duan Y, Wang J, Cai J, et al. (2022) The leucine-rich repeat (LRR) domain of NLRP3 is required for NLRP3 inflammasome activation in macrophages. *J Biol Chem* 298: 102717. https://doi.org/10.1016/j.jbc.2022.102717
20. Xie Q, Liu Y, Li X (2020) The interaction mechanism between autophagy and apoptosis in colon cancer. *Transl Onco*l 13: 100871. https://doi.org/10.1016/j.tranon.2020.100871
21. Qin ZH (2019) Autophagy: Biology and Diseases: Basic Science, 1st ed., Springer, Singapore.
22. Filomeni G, de Zio D, Cecconi F (2015) Oxidative stress and autophagy: The clash between damage and metabolic needs. *Cell Death Differ* 22: 377–388. https://doi.org/10.1038/cdd.2014.150
23. Zhang C, Luo X, Chen J, et al. (2019) Osteoprotegerin promotes liver steatosis by targeting the ERK-PPAR-γ-CD36 pathway. *Diabetes* 68: 1902–1914. https://doi.org/10.2337/db18-1055
24. Pancer Z, Cooper MD (2006) The evolution of adaptive immunity. *Annu Rev Immuno*l 24: 497–518. https://doi.org/10.1146/annurev.immunol.24.021605.090542
25. Burotto M, Chiou VL, Lee JM, et al. (2014) The MAPK pathway across different malignancies:

A new perspective. *Cancer* 120: 3446–3456. https://doi.org/10.1002/cncr.28864
26. Lombardo GE, Lepore SM, Morittu VM, et al. (2018) Effects of oleacein on high-fat diet-dependent steatosis, weight gain, and insulin resistance in mice. *Front Endocrinol (Lausanne)* 9: 116. https://doi.org/10.3389/fendo.2018.00116
27. Wu L, Zhang S, Zhang Q, et al. (2024) The molecular mechanism of hepatic lipid metabolism disorder caused by $NaAsO_2$ through Regulating the ERK/PPAR signaling pathway. *Oxid Med Cell Longev*: 9847073. https://doi.org/10.1155/2024/9847073
28. Xu WN, Chen DH, Liu WB, et al. (2018) Molecular characterization of microtubule-associated protein 1-light chain 3B in Megalobrama amblycephala fed with high fat/berberine diets. *J Appl Genet* 59: 345–355. https://doi.org/10.1007/s13353-018-0451-8
29. Lu KL, Wang LN, Zhang DD, et al. (2017) Berberine attenuates oxidative stress and hepatocytes apoptosis via protecting mitochondria in blunt snout bream Megalobrama amblycephala fed high-fat diets. *Fish Physiol Biochem* 43: 65–76. https://doi.org/10.1007/s10695-016-0268-5
30. Chen CZ, Chai Y, Wang YJ, et al. (2023) Physiological and molecular responses in the silver carp (*Hypophthalmichthys molitrix*) larvae after acute mercury exposure. *Environ Sci Pollut Res* 30: 49760–49770. https://doi.org/10.1007/s11356-023-25842-8
31. Buettner GR (2011) Superoxide dismutase in redox biology: the roles of superoxide and hydrogen peroxide. *Anti-cancer Agents Med Chem* 11: 341–346. https://doi.org/10.2174/187152011795677544
32. Ma X, Chen Z, Wang L, et al. (2018) The pathogenesis of diabetes mellitus by oxidative stress and inflammation: its inhibition by berberine. *Front Pharmacol* 9: 782. https://doi.org/10.3389/fphar.2018.00782
33. Zhao Y, Hu X, Liu Y, et al. (2017) ROS signaling under metabolic stress: Cross-talk between AMPK and AKT pathway. *Mol Cancer* 16: 79. https://doi.org/10.1186/s12943-017-0648-1
34. Raza MH, Siraj S, Arshad A, et al. (2017) ROS-modulated therapeutic approaches in cancer treatment. *J Cancer Res Clin Oncol* 143: 1789–1809. https://doi.org/10.1007/s00432-017-2464-9
35. Bortner CD, Cidlowski JA (1998) A necessary role for cell shrinkage in apoptosis. *Biochem Pharmacol* 56: 1549–1559. https://doi.org/10.1016/s0006-2952(98)00225-1
36. Lindenboim L, Zohar H, Worman HJ, et al. (2020) The nuclear envelope: Target and mediator of the apoptotic process. *Cell Death Discov* 6: 29. https://doi.org/10.1038/s41420-020-0256-5
37. Chen H, Xiang Y, Yin Y, et al. (2021) The m6A methyltransferase METTL3 regulates autophagy and sensitivity to cisplatin by targeting ATG5 in seminoma. *Transl Androl Urol* 10: 1711–1722. https://doi.org/10.21037/tau-20-1411
38. Levine B, Klionsky D (2004) Development by self-digestion: Molecular mechanisms and biological functions of autophagy. *Dev Cell* 6: 463–477. https://doi.org/10.1016/S1534-5807(04)00099-1
39. Kunapuli P, Chitta KS, Cowell JK (2003) Suppression of the cell proliferation and invasion phenotypes in glioma cells by the LGI1 gene. *Oncogene* 22: 3985–3991. https://doi.org/10.1038/sj.onc.1206584
40. Shen HM, Liu Z (2006) JNK signaling pathway is a key modulator in cell death mediated by reactive oxygen and nitrogen species. *Free Radic Biol Med* 40: 928–939. https://doi.org/10.1016/j.freeradbiomed.2005.10.056
41. Liu T, Chen XM, Sun JY, et al. (2018) Palmitic acid-induced podocyte apoptosis via the reactive oxygen species-dependent mitochondrial pathway. *Kidney Blood Press Re*s 43: 206–219.

https://doi.org/10.1159/000487673
42. Hsieh MJ, Tsai TL, Hsieh YS, et al. (2013) Dioscin-induced autophagy mitigates cell apoptosis through modulation of PI3K/Akt and ERK and JNK signaling pathways in human lung cancer cell lines. *Arch Toxicol* 87: 1927–1937. https://doi.org/10.1007/s00204-013-1047-z
43. Zhang L, Wang H, Zhu J, et al. (2014) Mollugin induces tumor cell apoptosis and autophagy via the PI3K/AKT/mTOR/p70S6K and ERK signaling pathways. *Biochem Bio phys Res Commun* 450: 247–254. https://doi.org/10.1016/j.bbrc.2014.05.101
44. Wang Y, Zhang H (2019) Regulation of autophagy by mTOR signaling pathway. *Adv Exp Med Biol* 1206: 67–83. https://doi.org/10.1007/978-981-15-0602-4_3

AIMS Press